

CO₂ STRIPPING FROM DIETHANOLAMINE USING MEMBRANE CONTACTORS: MODEL VALIDATION AND MEMBRANE WETTABILITY

H. N. Mohammed^{a*}, Omar S. Lateef^a, Ghassan H. Abdullah^a, A. L. Ahmad^b

^aDepartment of Chemical Engineering, Tikrit University, Saladin, Iraq

^bSchool of Chemical Engineering, Engineering Campus, Universiti Sains Malaysia, 14300 Nibong Tebal, Pulau Pinang, Malaysia

Article history

Received

20 June 2018

Received in revised form

11 June 2019

Accepted

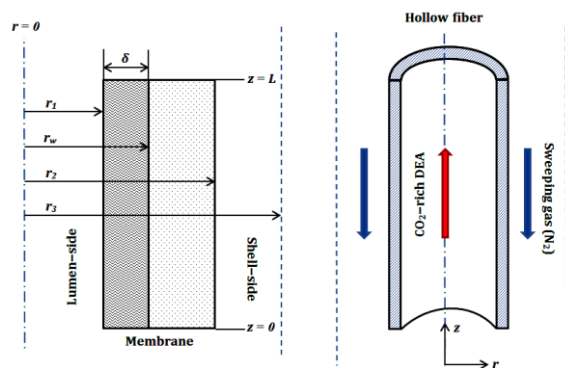
1 August 2019

Published online

24 October 2019

*Corresponding author
hnmohammed@tu.edu.iq

Graphical abstract



Abstract

CO₂ has been considered as the main greenhouse gas that contributes to global warming. Recently, membrane gas-liquid contactors are considered as alternative technique for gas absorption/desorption instead of conventional column. One of the undesirable features for this technique is the membrane wettability. In the present work, CO₂ desorption (stripping) from diethanolamine (DEA) solution using polyvinylidene fluoride hollow fiber membrane contactor is theoretically investigated. A comprehensive two dimensional mathematical model is developed to evaluate the membrane wettability when DEA solution is used at different operating conditions such as sweeping gas flow rate, initial CO₂ loading, liquid phase temperature and flow rate of liquid phase. The model results revealed that the effect of sweeping gas flow rate on the stripping flux was negligible. In contrast, CO₂ stripping flux was proportionally increased when the temperature and liquid phase flow rate were increased. In addition, the simulated results were compared with the experimental data obtained from literature which were in good agreement. Moreover, the results revealed that the PVDF membrane was suffered from wetting at studied operating conditions.

Keywords: CO₂ stripping, mathematical modeling, diethanolamine, membrane contactors, wetting mode

Abstrak

CO₂ merupakan sumber gas utama untuk fenomena rumah hijau yang menyebabkan kepada pemanasan global. Terkini, kaedah penyentuh gas-cecair membran merupakan langkah alternatif untuk penyerapan gas-nyahserapan bukan setakat terus lazim. Namun kebasahan membran merupakan salah satu sifat yang tidak diingini dalam kaedah ini. Dalam kajian ini, nyahserapan CO₂ daripada larutan diethanolamina (DEA) menggunakan penyentuh gantian geronggang dikaji secara teorinya. Satu model matematik dua dimensi menyeluruh dibangunkan untuk menilai kebasahan membran apabila larutan DEA pada keadaan berbeza digunakan seperti kadar aliran gas yang menyapu, muatan awal CO₂, suhu fasa cecair dan kadar aliran fasa cecair. Hasil model menunjukkan kesan kadar aliran gas yang menyapu pada fluks pelucutan tidak dapat diabaikan. Sebaliknya, fluks pelucutan CO₂ meningkat secara berkadar terus dengan suhu

dan juga kadar aliran larutan. Tambahan itu, keputusan simulasi dibandingkan dengan data eksperimen daripada kajian kesusasteraan menunjukkan padanan yang bersesuaian. Selain itu, hasil kajian membran PVDF yang mengalami kebasahan pada keadaan operasi turut dikaji.

Kata kunci: Pelucutan CO₂, model matematik, diethanolamine, gentian geronggang, mod kebasahan

© 2019 Penerbit UTM Press. All rights reserved

1.0 INTRODUCTION

Greenhouse gases, mainly carbon dioxide (CO₂), have been demonstrated recently to be significantly contributed to global warming [1]. The CO₂ emission to the atmosphere is increased due to the growing of industrial activities, mainly the consuming of fossil fuels in power plants [2]. Absorption method is deemed as the most promising technology for CO₂ recovery from flue gas streams [3, 4]. Aqueous solutions of amines such as monoethanolamine (MEA), diethanolamine (DEA) and methyl-diethanolamine (MDEA) are broadly used as a solvent for CO₂ removal from flue gas and natural gas streams [5].

Conventional equipment (packed and bubble columns) are used in the absorption process involving operating problems such as flooding, loading, foaming and channelling [6]. Membrane contactors are proposed in the past few decades as an alternative technique to overcome the conventional equipment disadvantages [7, 8]. Polymeric membranes with hydrophobic property are widely used in membrane contactors such as poly(tetrafluoroethylene) (PTFE), poly(vinylidene fluoride) (PVDF) and polypropylene (PP) [9, 10].

Besides, the membrane contactors are used in CO₂ stripping process to regenerate the CO₂-rich solvent that leaves absorption equipment. Experimental studies were performed to evaluate CO₂ stripping performance in membrane contactors [11, 12]. Simioni *et al.* [13] have reported an experimental work of CO₂ desorption from solution of potassium carbonate with concentration of 30% (w/w) using membrane contactor. They used flat sheet membranes of PTFE and an asymmetric polyethersulfone. The asymmetric membrane was coated with hydrophobic layer. The experiments were performed at temperatures range of 60-100°C. They observed that PTFE membrane performance is not well at higher temperatures. They pointed out that PTFE membrane performance is due to the penetration of solvent into membrane pores. Therefore, membrane wettability is a significant factor that determines the CO₂ stripping rate in gas-liquid membrane contactors.

Theoretical studies were performed to simulate CO₂ stripping using gas-liquid membrane contactors. A mathematical model was proposed by

Mehdipourghazi *et al.* [14] to simulate the CO₂ stripping from water using PVDF membrane contactor. They developed their model based on an assumption that gas occupies the pores of membrane (non-wetting mode). The predicted results were in good agreement with experimental data obtained from literature for studied range of liquid velocity and liquid temperature with a maximum error of 6%. Ghadiri *et al.* [15] proposed a 2D-mathematical model based on non-wetting-mode assumption to simulate desorption of CO₂ from MEA aqueous solution using PTFE membrane contactor. They pointed out that the model results showed good agreement with the experimental data. However, polymeric membranes suffer from wetting when employing alkanolamine aqueous solutions as CO₂ absorbent [16-19].

To our best knowledge, there is no mathematical model in the open literature is performed to simulate CO₂ stripping from amine solution taking into account the membrane wetting impact. Accordingly, this work is aimed to develop a comprehensive mathematical model to evaluate the effect of membrane wetting on CO₂ stripping using membrane contactor of hydrophobic PVDF hollow fiber membrane. DEA solution is adopted as common CO₂ solvent in absorption-desorption process. The influence of membrane wetting on the CO₂ stripping rate is investigated through different operating conditions such as liquid flow and sweeping gas flow rates, absorbent liquid temperature, and the initial loading of CO₂ in amine solution. The model results are validated with the experimental data reported by Abdul Rahim *et al.* [20].

2.0 MATHEMATICAL MODEL DEVELOPMENT

The membrane contactor consists of three domains: lumen-(tube)-side, membrane-side, and shell-side. In the CO₂ stripping process, CO₂-rich aqueous DEA solution flows through lumen side, while N₂ gas as a sweeping gas (carrier gas) flows through shell side in a counter-current configuration as shown in Figure 1. The released CO₂ molecules from DEA solution will be diffused from lumen side to shell side through membrane pores. Developing of 2D-dimensional mathematical model was performed in order to

predict CO₂ transfer through HFMC when using it in CO₂ stripping process. Reasonable assumptions were considered as follows: (1) the system at steady-state condition; (2) the flow inside the lumen side is a laminar fully developed flow; (3) the temperature in all domains of the contactor is constant (isothermal); and (4) is the gas-liquid interface is represented by Henry's law.

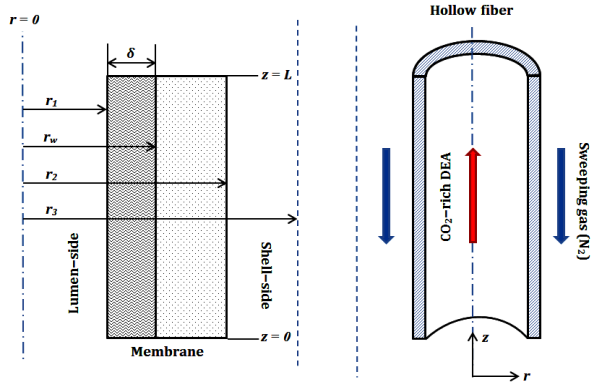


Figure 1 Schematic diagrams of the hollow fiber membrane contactor

2.1 Material Balance

Based on aforementioned assumptions, material balance has been conducted for each species that are transferred in membrane module to generate the mathematical model equations.

2.1.1 Tube Side

The species in the tube side, CO₂ and DEA, are diffused by both molecular and convective diffusion. Accordingly, continuity equations involving chemical reaction term can be written as follows:

$$D_{CO_2-tube} \left[\frac{\partial^2 C_{CO_2-tube}}{\partial r^2} + \frac{1}{r} \frac{\partial C_{CO_2-tube}}{\partial r} \right] - R_{CO_2} = v_{z-tube} \frac{\partial C_{CO_2-tube}}{\partial z} \quad (1)$$

$$D_{DEA-tube} \left[\frac{\partial^2 C_{DEA-tube}}{\partial r^2} + \frac{1}{r} \frac{\partial C_{DEA-tube}}{\partial r} \right] - R_{DEA} = v_{z-tube} \frac{\partial C_{DEA-tube}}{\partial z} \quad (2)$$

where R_{CO_2} and R_{DEA} are chemical reaction rates for CO₂ and DEA, respectively which are functions of CO₂ and DEA concentrations. The axial velocity distribution in tube side can be expressed as:

$$v_{z-tube} = 2 \bar{v}_{z-tube} \left[1 - \left(\frac{r}{r_1} \right)^2 \right] \quad (3)$$

The boundary conditions for each species in the membrane tube side can be written as:

$$\begin{aligned} \text{at } z = 0, C_{CO_2-tube} &= C_{CO_2-tube(in)}, C_{DEA} \\ &= C_{DEA-tube(in)} \text{ (inlet condition)} \end{aligned} \quad (4)$$

$$\text{at } r = 0, \frac{\partial C_{CO_2-tube}}{\partial r} = \frac{\partial C_{DEA-tube}}{\partial r} = 0 \text{ (symmetry)} \quad (5)$$

$$\text{at } r = r_1, C_{CO_2-tube} = \frac{C_{CO_2-mem}}{H}, \frac{\partial C_{DEA-tube}}{\partial r} = 0 \quad (6)$$

where H is the dimensionless Henry's constant.

Non-wetting Mode

The CO₂ molecules are diffused through the membrane pores at non-wetting condition by molecular diffusion only. The continuity equation for CO₂ transportation through the microporous membrane with the absence of the axial molecular diffusion can be written as:

$$D_{CO_2-mem} \left[\frac{\partial^2 C_{CO_2-mem}}{\partial r^2} + \frac{1}{r} \frac{\partial C_{CO_2-mem}}{\partial r} \right] = 0 \quad (7)$$

The boundary conditions are:

$$\text{at } r = r_1, C_{CO_2-mem} = C_{CO_2-tube} \times H \quad (8)$$

$$\text{at } r = r_2, C_{CO_2-mem} = C_{CO_2-shell} \quad (9)$$

The diffusion coefficient of CO₂ in the membrane side (D_{CO_2-mem}) is represented by the effective diffusivity of CO₂ that is filled the membrane pores and its calculations as detailed in Appendix.

Partial-wetting Mode

The CO₂-rich solution may penetrate the pores of membrane due to low wetting resistance of membrane and therefore one portion of the membrane will fill with liquid while the other portion fills with gas, as presented in Figure 1. The material balance equation for each species transport in the wetted part of the membrane side may be written as:

$$D_{CO_2-mem-L} \left[\frac{\partial^2 C_{CO_2-mem-L}}{\partial r^2} + \frac{1}{r} \frac{\partial C_{CO_2-mem-L}}{\partial r} \right] - R_{CO_2} = 0 \quad (10)$$

$$D_{DEA-mem-L} \left[\frac{\partial^2 C_{DEA-mem-L}}{\partial r^2} + \frac{1}{r} \frac{\partial C_{DEA-mem-L}}{\partial r} \right] - R_{DEA} = 0 \quad (11)$$

The required boundary conditions are:

$$\begin{aligned} \text{at } r = r_1, C_{CO_2-mem-L} &= C_{CO_2-tube}, C_{DEA-mem-L} \\ &= C_{DEA-tube} \end{aligned} \quad (12)$$

$$\begin{aligned} \text{at } r = r_w, C_{CO_2-mem-L} &= \frac{C_{CO_2-mem-G}}{H}, \frac{\partial C_{DEA-mem-L}}{\partial r} \\ &= 0 \end{aligned} \quad (13)$$

where r_w is the radius of the liquid portion in the membrane side which can be calculated as:

$$r_w = r_1 + \delta \quad (14)$$

$$\delta = \frac{x}{100}(r_2 - r_1) \quad (15)$$

where δ and x are the thickness and percentage of the liquid portion in the membrane side, respectively. The diffusion coefficients in the liquid portion of the membrane may be obtained as:

$$D_{CO_2-mem-L} = \frac{\varepsilon}{\tau} D_{CO_2-tube} \quad (16)$$

$$D_{DEA-mem-L} = \frac{\varepsilon}{\tau} D_{DEA-tube} \quad (17)$$

In contrast, the material balance equation for CO₂ transport in the non-wetted part of the membrane side can be written as:

$$D_{CO_2-mem-G} \left[\frac{\partial^2 C_{CO_2-mem-G}}{\partial r^2} + \frac{1}{r} \frac{\partial C_{CO_2-mem-G}}{\partial r} \right] = 0 \quad (18)$$

The diffusion coefficient is obtained from the following:

$$D_{CO_2-mem-G} = \frac{\varepsilon}{\tau} D_{CO_2-shell} \quad (19)$$

The boundary conditions are:

$$\text{at } r = r_w, C_{CO_2-mem-G} = C_{CO_2-mem-L} \times H \quad (20)$$

$$\text{at } r = r_2, C_{CO_2-mem-G} = C_{CO_2-shell} \quad (21)$$

2.1.3 Shell Side

The CO₂ transportation in the shell side is progressively governed by the convection and molecular diffusion. Therefore, the continuity equations for the transport of both CO₂ and sweeping gas (N₂) in the shell side may be written as:

$$D_{CO_2-shell} \left[\frac{\partial^2 C_{CO_2-shell}}{\partial r^2} + \frac{1}{r} \frac{\partial C_{CO_2-shell}}{\partial r} \right] = v_{z-shell} \frac{\partial C_{CO_2-shell}}{\partial z} \quad (22)$$

$$D_{N_2-shell} \left[\frac{\partial^2 C_{N_2-shell}}{\partial r^2} + \frac{1}{r} \frac{\partial C_{N_2-shell}}{\partial r} \right] = v_{z-shell} \frac{\partial C_{N_2-shell}}{\partial z} \quad (23)$$

The shell side velocity distribution can be estimated according to Happel's model [21], as:

$$v_{z-shell} = 2\bar{v}_{z-shell} \left[1 - \left(\frac{r_2}{r_3} \right)^2 \right] \times \frac{(r/r_3)^2 - (r_2/r_3)^2 + \ln(r_2/r)}{3 + (r_2/r_3)^4 - 4(r_2/r_3)^2 + 4\ln(r_2/r_3)} \quad (24)$$

where \bar{v} is the shell-side average velocity and r_3 is the radius of the free surface which can be determined as:

$$r_3 = r_2 \left(\frac{1}{1-\phi} \right)^{1/2} \quad (25)$$

where ϕ is the module void volume fraction that can be calculated as:

$$1 - \phi = \frac{Nr_2^2}{R_s^2} \quad (26)$$

where N is the number of the hollow fibers in the membrane module, and R_s is the inner radius of the module shell.

at $z = L, C_{CO_2-shell} = 0, C_{N_2-shell}$

$$= C_{N_2-shell(in)} \text{ (inlet condition)} \quad (27)$$

$$\text{at } r = r_2, C_{CO_2-shell} = C_{CO_2-mem}, \frac{\partial C_{N_2-shell}}{\partial r} = 0 \quad (28)$$

$$\text{at } r = r_3, \frac{\partial C_{CO_2-shell}}{\partial r} = \frac{\partial C_{N_2-shell}}{\partial r} = 0 \text{ (symmetry)} \quad (29)$$

2.2 Chemical Reaction Kinetics

The reaction between CO₂ and amine is a reversible reaction which allows CO₂ to release (desorb) from CO₂-rich amine solution at a certain operating condition. The reaction rate equation represents an important term in mass balance equations. A second order reaction rate equation was successfully used in mathematical modeling for CO₂ absorption in MEA and NaOH solutions using membrane contactor [19, 22]. In case of CO₂ desorption from DEA, the adopted reaction rate is first order with respect to the reactants (CO₂ and DEA) [23], as shown below:

$$R_{CO_2} = k_{app}[CO_2][DEA] \quad (30)$$

$$R_{DEA} = 2k_{app}[CO_2][DEA] \quad (31)$$

where k_{app} is the apparent second-order rate constant was proposed by Zhang X. and Zhang [24] as

$$\ln k_{app} = 24.515 - \frac{5411.3}{T} \quad (32)$$

2.3 Physical Properties and Numerical Solution

To solve model equations, physical and chemical properties are required such as physical solubility of CO₂ in the DEA solution, diffusion coefficients for the gas and liquid phase which are listed in Table 1. The characteristics of the simulated HFMC module are presented in Table 2. The DEA concentration in aqueous solution is 0.5 M and the initial CO₂ loading is 0.495 mol/l. The generated model equations for tube, membrane and shell sides of the membrane module as solved with appropriate boundary conditions are solved using COMSOL Multiphysics software version 5.2. Finite elements method is adopted for numerical solution for set of differential equations.

Table 1 Physical and chemical properties

Property	Expression or specific value	Reference
D_{CO_2-tube} , m^2/s	$D_{N_2O-DEA} \left(\frac{D_{CO_2-water}}{D_{N_2O-water}} \right)$ 1.729	[25] (see Apendix)
$D_{DEA-tube}$, m^2/s	$\times 10^{-6} \exp \left(\frac{-2287.7}{T} - 19.699 \right)$ $\times 10^{-5} C_{DEA-tube}$	[26]
$D_{CO_2-shell}$, m^2/s	$7.774 \times 10^{-5} \frac{T^{1.75}}{P}$ (1.854 – 7.904)	[27]
H	$\times 10^{-5} C_{DEA-tube} \exp \left(-\frac{240}{T} \right)$	[25]

Table 2 Characteristic dimensions and properties of HFMC [20]

Parameter	value
Module inner diameter (D_s)	11 mm
Effective fiber length (L)	260 mm
Fiber inner radius (r_i)	0.21 mm
Fiber outer radius (r_2)	0.55 mm
Number of fibers (N)	10
Membrane pore diameter	602.3 nm
Membrane porosity (ϵ)	56.57%
Membrane tortuosity (τ)	3

3.0 RESULTS AND DISCUSSION

The CO_2 stripping flux (J_{CO_2}) was adopted to evaluate the impact of the studied operating conditions on the CO_2 stripping process using HFMC. It can be calculated from the following:

$$J_{CO_2} = \frac{(C_{CO_2-tube(in)} - C_{CO_2-tube(out)}) \times Q_l}{A_i} \quad (33)$$

where $C_{CO_2-tube(in)}$ and $C_{CO_2-tube(out)}$ are concentrations of carbon dioxide in the inlet and outlet regions of tube side of the module, respectively. Q_l is the volumetric flow rate of liquid solvent. A_i is the total area of inner surface of the fibers.

3.1 CO_2 Concentration Distribution in HFMC

The concentration distribution of CO_2 in all sections of HFMC for non-wetting ($x = 0$) and partial-wetting ($x = 50\%$) modes are represented in terms of the ratio of the local CO_2 concentration to its initial value (C/C_o), as illustrated in Figure 2. The CO_2 -rich DEA aqueous solution had the highest concentration at the entrance zone of the tube-side of membrane (at $z = 0$). In contrast, it equals to zero at the entrance zone of the shell-side of the membrane (at $z = L$). It can be also observed that the CO_2 concentration in tube-side has depletion in the axial direction when the CO_2 -rich solution moves away from the entrance

zone. This is because that the CO_2 molecules are diffuse through membrane pores in present of concentration gradient. Moreover, Figure 2 shows that CO_2 concentration ratio varies greatly at the gas/liquid interface for $r = r_i$ (non-wetting) and $r = r_w$ (partial-wetting) with a slight change of CO_2 concentration near the axis of HFMC ($r = 0$). This could attribute to two facts: the CO_2 desorption rate (backward reaction rate) is faster than the CO_2 diffusion rate in the liquid phase and the CO_2 desorption only accure at the gas/liquid interface [28].

The CO_2 concentration distribution (C/C_o) in the radial direction (r/r_3) for both non-wetting and partial-wetting modes are presented in Figure 3. It can be clearly observed that CO_2 concentration was sharply declined in tube-side and liquid portion of the membrane for partial-wetting mode compared to concentration gradient in the gas phase of the membrane and shell sides. This is because of the CO_2 diffusion coefficient in the liquid phase is smaller than the diffusion coefficient in the gas phase.

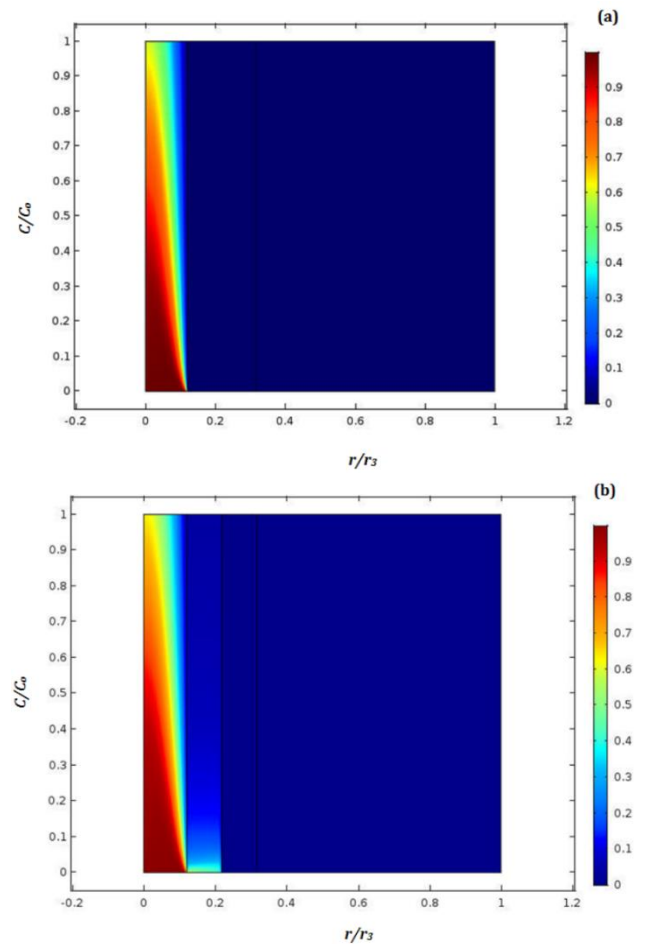


Figure 2 Distribution of CO_2 concentration in HFMC for (a) non-wetting mode; (b) partial-wetting mode, $x = 50\%$. ($Q_l = 50$ ml/min, $Q_g = 600$ ml/min and $T = 60^\circ C$)

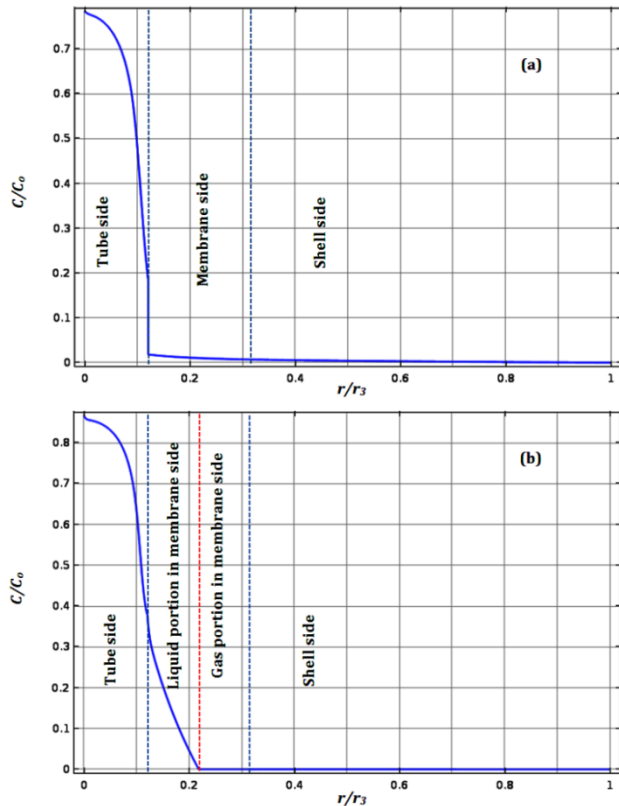


Figure 3 Distribution of CO₂ concentration in radial direction of the HFMC at the distance of $z/L = 0.25$ (a) non-wetting mode; (b) partial-wetting mode, $x = 50\%$. ($Q_l = 50$ ml/min, $Q_g = 600$ ml/min and $T = 60^\circ\text{C}$)

3.2 Effect of Operating Conditions and Model Validation

3.2.1 Effect of Liquid Flow Rate

The effect of liquid flow rate on CO₂ stripping performance at non-wetting and partial-wetting modes is illustrated in Figure 4. As presented, the CO₂ stripping flux is proportionally increases with an increase in liquid phase flow rate. A similar result was obtained by Naim *et al.* [13], Ghadiri *et al.* [15], and Masoumi *et al.* [29]. This behaviour may attribute to the reducing in liquid phase mass transfer resistance due to the reducing in the liquid boundary layer thickness when liquid flow rate is increased. On the other hand, a decline in the CO₂ stripping flux can be clearly observed when the membrane is switched from non-wetting to partial-wetting mode; as well the stripping flux continuously decreases with an increase in the wetting fraction value. This is because that DEA solution penetrates through the membrane pores which leads to increase the membrane side mass transfer resistance and hence decreases the CO₂ stripping flux [22].

Figure 5 illustrates the effect of liquid flow rate on the distribution of CO₂ concentration in the tube side. It can clearly observe that the concentration distribution of CO₂ changes when the liquid flow rate change. Moreover, the decline in CO₂ concentration

along the contactor is negligible at the high liquid flow rate. This could be due to the decreasing in residence time of CO₂ in the lumen side when the liquid flow rate increase which leads to decrease the mass transfer rate. The CO₂ stripping flux is increased 3.5 times in non-wetting mode when the liquid flow rate increased from 10 to 30 ml/min due to decrease the mass transfer resistance as aforementioned which significantly enhance the mass transfer rate. In contrast, the CO₂ stripping flux is only increased 1.5 times when the liquid flow rate varied from 40 to 100 ml/min because the CO₂ in the lumen side does not have enough time for mass transfer.

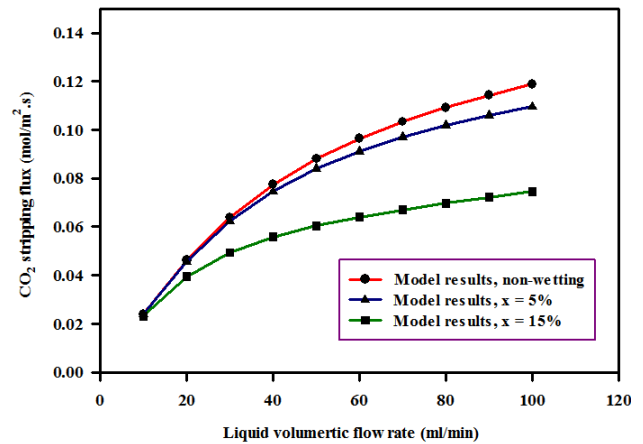


Figure 4 Effect of the liquid flow rate on the CO₂ stripping flux at different wetting modes ($Q_g = 600$ ml/min and $T = 90^\circ\text{C}$)

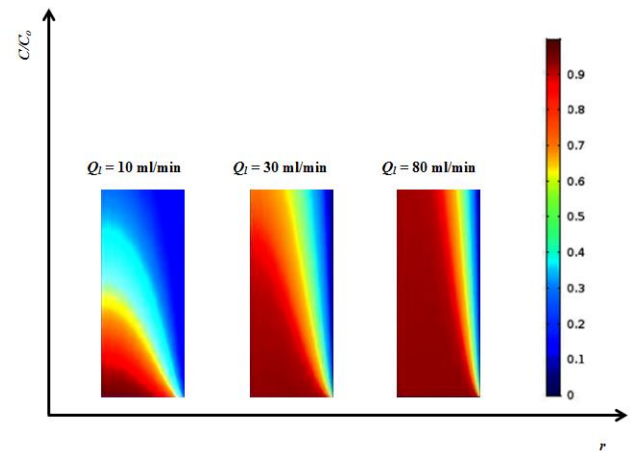


Figure 5 Effect of the liquid flow rate on the concentration distribution of CO₂ in the lumen side for the non-wetting mode ($Q_g = 600$ ml/min and $T = 90^\circ\text{C}$)

3.2.2 Effect of Sweeping Gas Flow Rate

Figure 6 shows effect of sweeping gas flow rate on CO₂ stripping flux for experimental and model results. As presented, the gas flow rate has an insignificant impact on the CO₂ desorption wherein the CO₂ stripping flux remains almost constant over a wide range of gas flow rates. This could be attributed to

the diminishing of gas phase mass transfer resistance at that the high gas flow rate. Consequently, the liquid phase and membrane mass transfer resistances may dominate the CO₂ desorption. Khaisri *et al.* [30] pointed out that the mass transfer resistance in liquid phase is about 90% of the total mass transfer resistance of HFMC. On the other hand, the model results exhibited that 5% wetting percentage had the best validity with the experimental data. This finding provides an evidence that membrane was suffering from wetting during the desorption process at the studied operating conditions. One of the desirable features of CO₂ solvent in HFMC is the high enough surface tension value. Solvent with low surface tension value could increase of penetration of liquid into membrane pores [1]. Moreover, the surface tension of amine solutions decreases with increase temperature of solution [31]. Consequently, the relatively high DEA aqueous solution temperature (60°C) may increase the possibility of the membrane to wet.

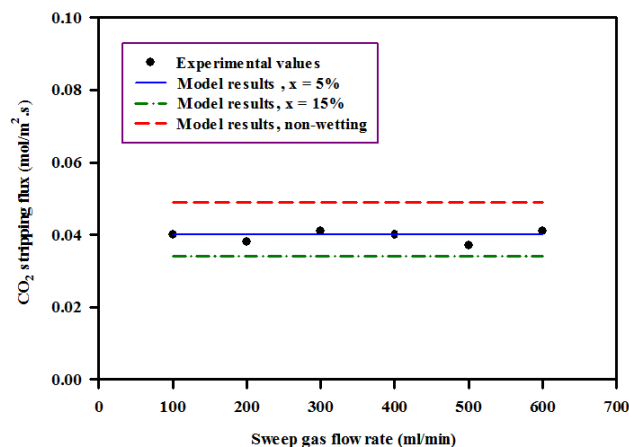


Figure 6 Effect of the gas flow rate on the CO₂ stripping flux at different wetting modes ($Q_l = 40$ ml/min and $T = 60^\circ\text{C}$). Experimental data were obtained from Abdul Rahim *et al.* [20]

3.2.3 Effect of Temperature

The effect of the liquid phase temperature on the CO₂ desorption flux was illustrated in Figure 7. Obviously, CO₂ stripping flux directly increases with an increase in amine solution temperature for both experimental and model results. This attributed to the reducing in solubility of CO₂ when amine temperature was increased. The CO₂ equilibrium partial pressure may increase also which increase the driving force towards the CO₂ desorption from the amine solution [27]. CO₂ stripping performance is declined at the low temperature and high liquid flow rate. This is because that an amount of CO₂ released in liquid phases is small due to the low temperature of the liquid; as well the high liquid flow rate provides an insufficient residence time for CO₂ molecules to diffuse through the liquid boundary layer. In contrast, the CO₂ stripping performance improves when the

temperature and liquid flow rate increase. A large amount of CO₂ molecules could release in liquid phase due to the high liquid temperature which can diffuse readily through the low resistance of the liquid boundary layer which generated by high liquid flow rate condition [32]. The model results showed that wetting percentage of 7% had a good agreement with the experimental data. Furthermore, CO₂ stripping flux at the non-wetting mode is higher than partial-wetting mode due to an increase in the mass transfer resistance in the membrane side when the liquid penetrates membrane pores.

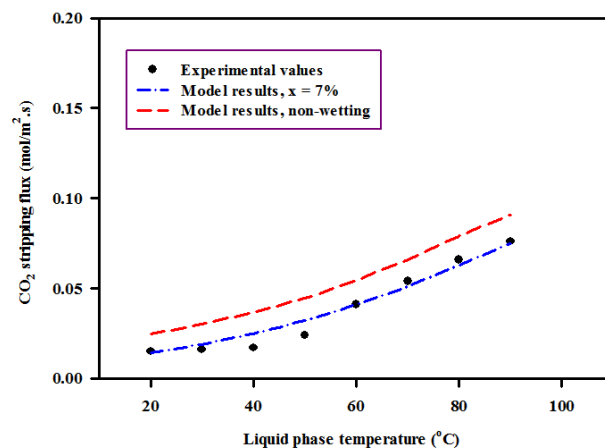


Figure 7 Effect of the liquid phases temperature on the CO₂ stripping flux at different wetting modes ($Q_l = 50$ ml/min and $Q_g = 600$ ml/min). Experimental data were obtained from Abdul Rahim *et al.* [20]

3.2.3 Effect of Initial CO₂ Loading Value

Figure 8 illustrates the effect of initial CO₂ loading in the DEA solution on CO₂ concentration at exit zone of the tube side of HFMC. Obviously, the outlet CO₂ concentration increases with an increase in initial CO₂ loading. The predicted outlet CO₂ concentrations at non-wetting mode for studied initial CO₂ loading were lower than the experimental data obtained from the literature. In contrast, the model results of $x = 7\%$ have good agreement with the experimental data compared to the non-wetting mode results. This finding provides an evidence that DEA solution has an ability to penetrate membrane pores at different initial CO₂ loading values. Model results at non-wetting mode have small difference with experimental data at low initial CO₂ loading. A decreasing in driving force for mass transfer of CO₂ could be occurred at low initial CO₂ loading values which reduces the axial and radial diffusion of CO₂ molecules vice versa with high initial CO₂ loading values.

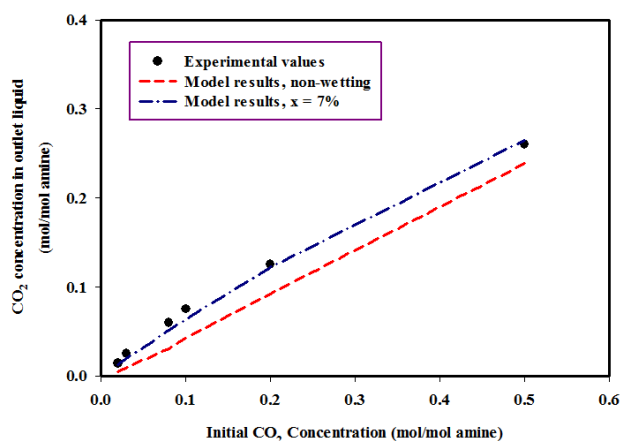


Figure 8 Effect of initial CO₂ loading on CO₂ concentration in outlet liquid stream of the module ($Q_l = 20$ ml/min, $Q_g = 600$ ml/min and $T = 100^\circ\text{C}$). Experimental data were obtained from Abdul Rahim *et al.* [20]

4.0 CONCLUSION

Two-dimensional mathematical model were developed to simulate mass transfer of CO₂ in stripping process using HFMC. Non-wetting and partial-wetting modes were considered in this model. The effect of operating conditions on the performance of desorption process were assessed in term of CO₂ stripping flux. It was observed that the major resistance is the liquid phase mass transfer resistance and accordingly the CO₂ stripping flux is increased with an increase in the liquid flow rate. In contrast, the sweeping gas flow rate has insignificant effect on the stripping flux. Moreover, the membrane has considerable wetting fractions which lead to decline the CO₂ stripping flux at the studied operating conditions. In addition, the CO₂ stripping flux increases when the liquid phase temperature increases. The simulation results were in a good agreement with the experimental data obtained from literature.

References

- [1] Ahmad, A. L., Mohammed, H. N., Ooi, B. S., Leo, C. P. 2018. Membrane Wetting in Carbon Dioxide Absorption Process Using Membrane Contactors: A Review. *Environmental Engineering & Management Journal*. 17(3): 723-738.
- [2] Yu, K. M. K., Curcic, I., Gabriel, J., Tsang, S. C. E. 2008. Recent Advances in CO₂ Capture and Utilization. *ChemSusChem* 2008. 1(11): 893-899. DOI: 10.1002/cssc.200800169
- [3] Wang, M., Lawal, A., Stephenson, P., Sidders, J., and Ramshaw, C. 2011. Post-Combustion CO₂ Capture with Chemical Absorption: A State-of-the-art Review. *Chemical Engineering Research and Design*. 89(9): 1609-1624. DOI: <https://doi.org/10.1016/j.cherd.2010.11.005>.
- [4] Kohl, A. L., and Riesenfeld, F. C. 1985. *Gas Purification*. Fourth ed. Gulf Publishing, Houston, TX, USA.
- [5] deMontigny, D., Tontiwachwuthikul, P., and Chakma, A. 2005. Comparing the Absorption Performance of Packed Columns and Membrane Contactors. *Industrial & Engineering Chemistry Research*. 44(15): 5726-5732.

- DOI: 10.1021/ie040264k.
- [6] Mosadegh-Sedghi, S., Rodrigue, D., Brisson, J., and Iliuta, M. C. 2014. Wetting Phenomenon in Membrane Contactors – Causes and Prevention. *Journal of Membrane Science*. 452: 332-353. DOI: <https://doi.org/10.1016/j.memsci.2013.09.055>.
- [7] Naim, R., Ismail, A. F., and Mansourizadeh, A. 2012. Preparation of Microporous PVDF Hollow Fiber Membrane Contactors for CO₂ Stripping from Diethanolamine Solution. *Journal of Membrane Science*. 392-393: 29-37. DOI: <https://doi.org/10.1016/j.memsci.2011.11.040>.
- [8] Abdulhameed, M. A., Othman, M. H. D., Ismail, A. F., Matsuura, T., Harun, Z., Rahman, M. A., Puteh, M. H., Jaafar, J., Rezaei, M., Hubadillah, S. K. 2017. Carbon Dioxide Capture Using a Superhydrophobic Ceramic Hollow Fibre Membrane for Gas-liquid Contacting Process. *Journal of Cleaner Production*. 140(Part 3): 1731-1738. DOI: <https://doi.org/10.1016/j.jclepro.2016.07.015>.
- [9] Mohammed, H. N., Ahmad, A. L., Ooi, B. S., Leo, C. P. 2014. CO₂ Absorption in Membrane Contactor using Piperazine, Monoethanolamine and Diethanolamine: A Mass Transfer and Performance Study. *Jurnal Teknologi (Sciences & Engineering)*. 69(9): 19-22. DOI: <https://doi.org/10.11113/jt.v69.3390>.
- [10] Ahmad, A. L., Mohammed, H. N., Ooi, B. S., Leo, C. P. 2013. Deposition of a Polymeric Porous Superhydrophobic Thin Layer on the Surface of Poly(vinylidene fluoride) Hollow Fiber Membrane. *Polish Journal of Chemical Technology*. 15(3): 1-6. DOI: 10.2478/pjct-2013-0036.
- [11] Liang, W., Chenyang, Y., Bin, Z., Xiaona, W., Zijun, Y., Lixiang, Z., Hongwei, Z., Nanwen, L. 2019. Hydrophobic Polyacrylonitrile Membrane Preparation and Its Use in Membrane Contactor for CO₂ Absorption. *Journal of Membrane Science*. 569: 157-165. DOI: <https://doi.org/10.1016/j.memsci.2018.09.066>.
- [12] Rahbari-Sisakht, M., Ismail, A.F., Rana, D., and Matsuura, T. 2013. Carbon Dioxide Stripping from Diethanolamine Solution Through Porous Surface Modified PVDF Hollow Fiber Membrane Contactor. *Journal of Membrane Science*. 427: 270-275. DOI: <https://doi.org/10.1016/j.memsci.2012.09.060>.
- [13] Simioni, M., Kentish, S. E., and Stevens, G. W. 2011. Membrane Stripping: Desorption of Carbon Dioxide from Alkali Solvents. *Journal of Membrane Science*. 378(1-2): 18-27. DOI: <https://doi.org/10.1016/j.memsci.2010.12.046>.
- [14] Mehdipourghazi, M., Barati, S., and Varaminian, F. 2015. Mathematical Modeling and Simulation of Carbon Dioxide Stripping from Water using Hollow Fiber Membrane Contactors. *Chemical Engineering and Processing: Process Intensification*. 95: 159-164. DOI: <https://doi.org/10.1016/j.cep.2015.06.006>.
- [15] Ghadiri, M., Marjani, A., and Shirazian, S. 2013. Mathematical Modeling and Simulation of CO₂ Stripping from Monoethanolamine Solution using Nano Porous Membrane Contactors. *International Journal of Greenhouse Gas Control*. 13: 1-8. DOI: <https://doi.org/10.1016/j.ijggc.2012.11.030>.
- [16] Rangwala, H. A. 1996. Absorption of Carbon Dioxide into Aqueous Solutions using Hollow Fiber Membrane Contactors. *Journal of Membrane Science*. 112(2): 229-240. DOI: [https://doi.org/10.1016/0376-7388\(95\)00293-6](https://doi.org/10.1016/0376-7388(95)00293-6).
- [17] Lu, J. G., Zheng, Y. F., and Cheng, M. D. 2008. Wetting Mechanism in Mass Transfer Process of Hydrophobic Membrane Gas Absorption. *Journal of Membrane Science*. 308(1-2): 180-190. DOI: <https://doi.org/10.1016/j.memsci.2007.09.051>.
- [18] Rongwong, W., Jiratananon, R., and Atcharyawut, S. 2009. Experimental Study on Membrane Wetting in Gas-Liquid Membrane Contacting Process for CO₂ Absorption by Single and Mixed Absorbents. *Separation and Purification Technology*. 69(1): 118-125. DOI: <https://doi.org/10.1016/j.seppur.2009.07.009>.
- [19] Faiz, R., and Al-Marzouqi, M. 2010. CO₂ Removal from Natural Gas at High Pressure using Membrane Contactors:

- Model Validation and Membrane Parametric Studies. *Journal of Membrane Science*. 365(1-2): 232-241. DOI: <https://doi.org/10.1016/j.memsci.2010.09.004>.
- [20] Abdul Rahim, N., Ghasem, N., and Al-Marzouqi, M. 2014. Stripping of CO₂ from Different Aqueous Solvents using PVDF Hollow Fiber Membrane Contacting Process. *Journal of Natural Gas Science and Engineering*. 21: 886-893. DOI: <https://doi.org/10.1016/j.jngse.2014.10.016>.
- [21] Happel, J. 1959. Viscous Flow Relative to Arrays of Cylinders. *AIChE J.* 5: 174-177.
- [22] El-Naas, M. H., Al-Marzouqi, M., Marzouk, S. A., and Abdullatif, N. 2010. Evaluation of the Removal of CO₂ using Membrane Contactors: Membrane Wettability. *Journal of Membrane Science*. 350(1-2): 410-416. DOI: <https://doi.org/10.1016/j.memsci.2010.01.018>.
- [23] Kierzkowska-Pawlak, H., and Chacuk, A. 2010. Carbon Dioxide Removal from Flue Gases by Absorption/Desorption in Aqueous Diethanolamine Solutions. *Journal of the Air & Waste Management Association*. 60: 925-931. DOI: [10.3155/1047-3289.60.8.925](https://doi.org/10.1016/j.jhazmat.2013.01.083).
- [24] Zhang, X., and Zhang, C. F. A. 2002. Kinetics of Absorption of Carbon Dioxide into Aqueous Solution of MDEA Blended with DEA. *Industrial & Engineering Chemistry Research*. 41(5): 1135-1141. DOI: [10.1021/je00051a011](https://doi.org/10.1021/je00051a011).
- [25] Versteeg, G. F., and van Swaaij, W. P. M. 1988. Solubility and Diffusivity of Acid Gases (CO₂, N₂O) in Aqueous Alkanolamine Solutions. *Journal of Chemical & Engineering Data*. 33(1): 29-34. DOI: [10.1021/je00011a037](https://doi.org/10.1021/je00011a037).
- [26] Snijder, E. D., te Riele, M. J. M., Versteeg, G. F., and van Swaaij, W. P. M. 1993. Diffusion Coefficients of Several Aqueous Alkanolamine Solutions. *Journal of Chemical & Engineering Data*. 38(3): 475-480. DOI: [10.1021/je00011a037](https://doi.org/10.1021/je00011a037).
- [27] Perry, R. H., and Green, D. W. 1997. *Perry's Chemical Engineers' Handbook*. Seventh ed. Mc Graw-Hill, New York.
- [28] Wang, Z., Fang, M., Yu, H., Ma, Q., and Luo, Z. 2013. Modeling of CO₂ Stripping in a Hollow Fiber Membrane Contactor for CO₂ Capture. *Energy & Fuels*. 27(11): 6887-6898. DOI: [10.1021/ef401488c](https://doi.org/10.1021/ef401488c).
- [29] Masoumi, S., Rahimpour, M.R., and Mehdipour, M. 2016. Removal of Carbon Dioxide by Aqueous Amino Acid Salts using Hollow Fiber Membrane Contactors. *Journal of CO₂ Utilization*. 16: 42-49. DOI: <https://doi.org/10.1016/j.jcou.2016.05.008>.
- [30] Khaisri, S., deMontigny, D., Tontiwachwuthikul, P., and Jiraratananon, R. 2011. CO₂ Stripping from Monoethanolamine using a Membrane Contactor. *Journal of Membrane Science*. 376(1-2): 110-118. DOI: <https://doi.org/10.1016/j.memsci.2011.04.005>.
- [31] Va zquez, G., Alvarez, E., Rendo, R., Romero, E., and Navaza, J.M. 1996. Surface Tension of Aqueous Solutions of Diethanolamine and Triethanolamine from 25°C to 50°C. *Journal of Chemical & Engineering Data*. 41(4): 806-808. DOI: [10.1021/je960012t](https://doi.org/10.1021/je960012t).
- [32] Naim, R., and Ismail, A. F. 2013. Effect of Polymer Concentration on the Structure and Performance of PEI Hollow Fiber Membrane Contactor for CO₂ Stripping. *Journal of Hazardous Materials*. 250-251: 354-361. DOI: <https://doi.org/10.1021/jhazmat.2013.01.083>.
- [33] Han, J., Jin, J., Eimer, D.A., and Melaaen, M. C. 2012. Density of Water (1) + Dethanolamine (2) + CO₂ (3) and Water (1) + N-methyldiethanolamine (2) + CO₂ (3) from (298.15 to 423.15) K. *Journal of Chemical & Engineering Data*. 57(6): 1843-1850. DOI: [10.1021/je300345m](https://doi.org/10.1021/je300345m).
- [34] Goyal, N., Suman, S., and Gupta, S. K. 215. Mathematical Modelling of CO₂ Separation from Gaseous-mixture using a Hollow-fiber Membrane Module: Physical Mechanism and Influence of Partial-Wetting. *Journal of Membrane Science*. 474: 64-82. DOI: <https://doi.org/10.1016/j.memsci.2014.09.036>.
- [35] Korson, L., Hansen, W. D., and Miller, F. J. 1969. Viscosity of Water at Various Temperatures. *The Journal of Physical Chemistry*. 73(1): 34-39. DOI: [10.1021/j100721a006](https://doi.org/10.1021/j100721a006).
- [36] Reid, R. C., Prausnitz, J. M., and Sherwood, T. K. 1977. *The Properties of Gases and Liquids*. Third Ed. Mc Graw-Hill, New York.
- [37] Neufeld, P. D., Janzen, A. R., and Aziz, R. A. 1972. Empirical Equations to Calculate 16 of the Transport Collision Integrals $\Omega^{(l,s)*}$ for the Lennard-Jones (12-6) Potential. *The Journal of Chemical Physics*. 57(3): 1100-1102. DOI: <https://doi.org/10.1063/1.1678363>.